Journal of Alloys and Compounds 500 (2010) 211–214

Contents lists available at ScienceDirect

Journal of Alloys and Compounds

journal homepage: www.elsevier.com/locate/jallcom

Preparation of Fe-doped semiconductor NiZrSn

Fangfang Wang, Tadashi Fukuhara*, Kunihiko Maezawa

Department of Liberal Arts and Sciences, Toyama Prefectural University, Imizu, Toyama 939-0398, Japan

ARTICLE INFO

Article history:
Received 8 January 2010
Received in revised form 23 March 2010
Accepted 1 April 2010
Available online 5 May 2010

Keywords:
Spintronics
Half-Heusler compound
Dilute magnetic semiconductor
Electrical resistivity

ABSTRACT

Fe-doped NiZrSn polycrystalline ingots were prepared using arc melting method. Microstructure and electrical properties of the ingots were investigated. According to the EDX results, the solubility of Fe in the $C1_b$ phase of the NiZrSn is about 2% by arc melting method. The electrical resistivity of low Fe-doped NiZrSn shows semiconducting temperature dependence and the transport gap estimated from activation plot is about 80 meV.

1. Introduction

Within the last decade, many attempts have been made to prepare semiconducting compounds that also exhibit ferromagnetic properties in order to realize applications for semiconductor spintronics. The dilute magnetic semiconductor (DMS) is one of the potential materials for these applications.

For the $C1_b$ compounds (such as NiZrSn) with the space group $F\bar{4}3m$ (No. 216), electronic-structure calculation [1–3] and many experiments [4–8] indicate that the compounds with 18 valence electrons are semiconductors. These $C1_b$ semiconductors become attractive material for spintronics application because the crystal structure is similar to that of III–V and II–VI semiconductors, which are often used for electronic equipment in present.

The magnetic effects are roughly proportional to the concentration of the magnetic ions in the DMS prepared by magnetic elements-doped $C1_b$ semiconductors. Therefore, the solubility of magnetic elements in these $C1_b$ semiconductors is important. Mn, Cr, Cu and Sb-doped NiZrSn solid solutions were successfully prepared, and the physical properties were reported previously [9–11]. In this work, Fe-doped NiZrSn were prepared, the solubility of Fe in the $C1_b$ phase of these ingots was investigated, and the electrical properties were presented.

2. Experimental procedure

The ingots of Fe-doped NiZrSn with the nominal composition $NiZr_{1-x}Fe_xSn$ for $0 \le x \le 0.1$ were prepared using arc melting method. For preparing these ingots, high purity Fe (99.99%), Ni (99.999%), Zr (99.9%), and Sn (99.9999%) were used as starting materials, and about 2 g of constituent elements were melted in a water-cooled Cu crucible using an arc furnace in a high purity Ar atmosphere. To obtain homogeneity, an ingot was turned over and melted several times. Annealing was performed at 800 °C for 100 h in an evacuated quartz tube.

X-ray powder diffraction (XRD), the scanning electron microscopy (SEM), energy dispersive X-ray spectroscopy (EDX), and the electron probe micro-analyzer (EPMA) analyses were carried out for the obtained ingots. Electrical resistivity was measured by a conventional four-probe method using a rectangular rod cut by a spark cutter whose size was typically $0.2 \times 1 \times 5\ mm^3$.

3. Results and discussion

A small piece was taken from the arc-melted ingot, and crushed into fine powder to measure XRD. Fig. 1(a) shows a typical XRD pattern of Fe-doped NiZrSn. As shown in the figure, intensive peaks are all assigned based on the $C1_b$ structure. For all the samples, the similar XRD patterns are observed. Because the additional peaks are much weak comparing with the main peaks, it is difficult to analyze additional peaks to make sure the variety of impurity phase using full scale of XRD patterns. Therefore, the log scale of XRD patterns of ingots with $x = 0$, 0.02, 0.03, and 0.1 are shown in Fig. 1(b). The diffraction peaks of paramagnetic metal Ni_2ZrSn [12] (marked with ●) were observed in the XRD pattern of four samples. For non-doped NiZrSn, the weak peaks arising from metallic Zr_5Sn_3 [13] (marked with ○) appear around $2\theta = 33–37°$. When $x = 0.02$, the most weak peaks arising from Zr_5Sn_3 comparing with that of other ingots are observed, suggesting the least impurity phase. The new weak impurity peaks arising from $Ni_{2.5}Fe_{2.5}Sn_3$ (marked with □) appear when $x = 0.03$. For ingot with $x = 0.1$, the peaks of Zr_5Sn_3 disappear, whereas the intensity of peaks of $Ni_{2.5}Fe_{2.5}Sn_3$ becomes strong.

* Corresponding author.
E-mail address: fukuhara@pu-toyama.ac.jp (T. Fukuhara).

0925-8388/$ – see front matter © 2010 Elsevier B.V. All rights reserved.
doi:10.1016/j.jallcom.2010.04.005

Table 1
EDX results of Fe-doped NiZrSn with $x = 0$, 0.02, and 0.1.

		Compositions (at.%) (±0.05)				Fe concentration	Compounds
		Ni:	Zr:	Fe:	Sn		
$x = 0$	A	34.75	32.56	0.00	32.50	0%	NiZrSn
	B	4.02	44.83	0.00	51.15		Zr–Sn
	C	5.76	35.64	0.00	47.85		Zr–Sn
$x = 0.02$	A	33.64	33.40	0.70	32.26	~2.0%	Fe-doped NiZrSn
	B	32.97	35.16	0.75	31.02		Fe-doped NiZrSn
	C	1.80	56.08	0.00	58.96		Zr–Sn
$x = 0.1$	A	33.35	33.73	0.80	32.12	~2.0%	Fe-doped NiZrSn
	B	29.31	41.69	1.37	27.63		–
	C	36.23	0.67	23.13	39.97		Ni–Fe–Sn

A small plate was cut from each ingot, and the surface of the plate was polished for the microscopic observations. The SEM images of the polished surface of ingots with $x = 0$, 0.02, and 0.1 are shown in Fig. 2. For each sample, the composition of the matrix (denoted as A) and the secondary phase (denoted as B and C) is checked by EDX. The atom percent of all elements and Fe concentration in matrix are listed in Table 1. Where, Fe concentration is estimated using (Fe (at.%))/(Fe (at.%) + Zr (at.%)) × 100%. For non-doped NiZrSn, matrix possesses a composition of Ni:Zr:Sn ~ 1:1:1, suggesting the $C1_b$ structure. Meanwhile, a little of secondary phase, Zr–Sn compounds, are observed in non-doped NiZrSn. For Fe-doped ingots, the matrix also possesses a composition of Ni:Zr:Sn about 1:1:1. It suggests that the matrix of all samples exhibit a similar composition with the $C1_b$ structure due to the limited low Fe doped. As Table 1 shows, when $x = 0.02$, about 1.8% Fe is detected in the matrix of the sample. When $x = 0.025$ and 0.03, Fe concentration is about 2% as illustrated in Fig. 3(b). Although the ingot prepared from nominal composition with further Fe-rich doping content such as $x = 0.1$, the Fe concentration in the matrix is also about 2%. This value is expected to be the solubility limit of Fe in the matrix of NiZrSn prepared by arc melting method. In additional, as Table 1 shows, when $x = 0.02$, the secondary phase, Zr–Sn compound, is detected in sample. For the samples with $x = 0.025$ and 0.03, new secondary phase of $Ni_{2.5}Fe_{2.5}Sn_3$ appears according to the EDX results (not shown here). When $x = 0.1$, the amount of secondary phase $Ni_{2.5}Fe_{2.5}Sn_3$ increased, which is consistent with XRD results.

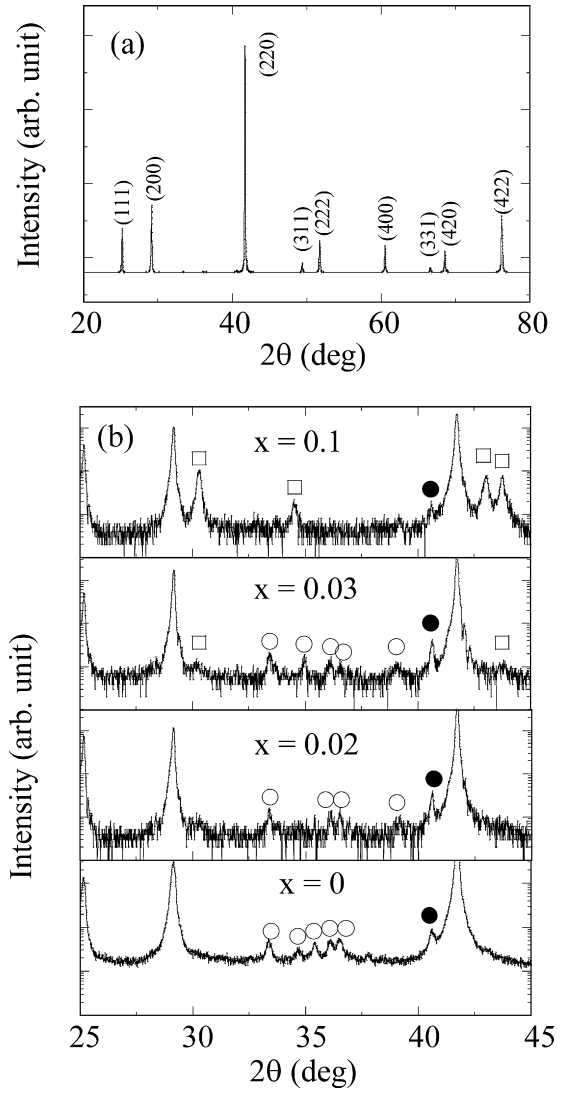

Fig. 1. (a) A typical XRD pattern of Fe-doped NiZrSn; (b) log scale of XRD patterns of ingots with $x = 0$, 0.02, 0.03 and 0.1. (●: Ni_2ZrSn, ○: Zr_5Sn_3, and □: $Ni_{2.5}Fe_{2.5}Sn_3$.)

Although the ingots were prepared from nominal composition as $NiZr_{1-x}Fe_xSn$, both of the EDX and EPMA results show a constant Zr content in the matrix of all samples, whereas, the concentration of Ni in the matrix shows a slight decreasing trend with increasing x. It suggests that the doped Fe ions in matrix trend to replace Ni rather than Zr. However, the details are not clear. Therefore, we cannot yet make clear whether Fe ions exactly replace Zr or Ni.

Fig. 3(a) shows x dependence of lattice constants estimated from the XRD patterns. The lattice constant decreases with increasing x from 0 to 0.03, it suggests that doped Fe ions substitutes for the atoms in the $C1_b$ structure of the samples. However, the lattice constant almost keeps a constant value when $x \geq 0.03$. As shown in Fig. 3(b), the Fe concentration in the $C1_b$ phase estimated from EDX results increases from 0 to about 2% as x increases from 0 to 0.03, and then almost saturates around 2% when $x \geq 0.03$. Fe concentration in the matrix for $x = 0.02$ and 0.10 ingots were also checked using EPMA analysis, which is more accurate than EDX analysis. As shown in Fig. 3(b), although the absolute value of Fe concentrations estimated by EPMA analysis is rather smaller than those estimated by EDX analysis, the overall behavior is consistent. Hence, the solubility limit of Fe in the $C1_b$ structure is more or less than 2%.

The electrical resistivity was measured using a rod cut from the plate examined by SEM. Fig. 4 shows the temperature dependence of electrical resistivity of ingots with $x = 0$, 0.02, and 0.025. The activation plot of sample with $x = 0.02$ is shown in the inset of Fig. 4. For these three samples, the resistivity increases with decreasing temperature, indicating obvious semiconducting behavior. However, when $x = 0$ and 0.025, the resistivity tends to saturated at low temperature, suggesting the existing of the metallic phases. At lower temperature, when the resistance of the matrix increases, the current flows selectively in such metallic path. Such behavior can cause the saturation of the resistivity. When $x = 0.02$, the resistivity con-

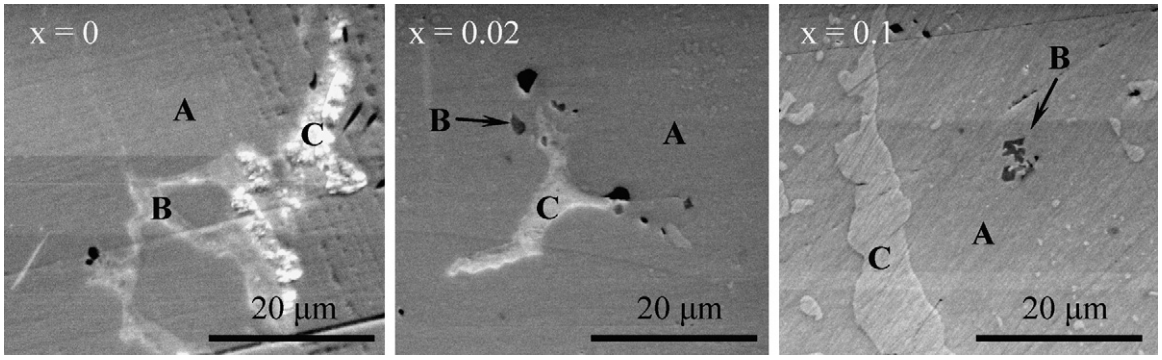

Fig. 2. SEM images of Fe-doped NiZrSn with $x = 0$, 0.02, and 0.1.

tinues to increase down to the lowest temperature, and the residual resistivity is twenty times larger than that of non-doped NiZrSn and ten times larger than that of the sample with $x = 0.025$ at the lowest temperature. It suggests the smallness of metallic segregation for the sample with $x = 0.02$.

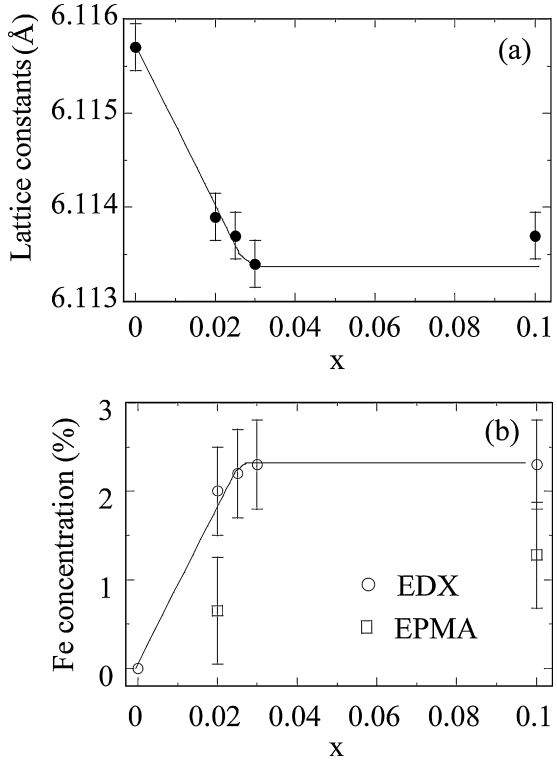

Fig. 3. (a) x dependence of lattice constant of Fe-doped NiZrSn; (b) x dependence of Fe concentration estimated from EDX results. Solid lines are guides to the eye.

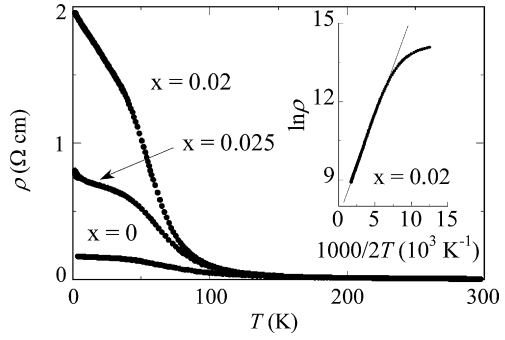

Fig. 4. Temperature dependence of electrical resistivity of Fe-doped NiZrSn with $x = 0$, 0.02, and 0.025. Inset: Activation plot of ingot with $x = 0.02$.

The resistivity of sample with $x \sim 0.02$ seems to reflect the semiconducting nature of the matrix. As shown in the inset of Fig. 4, above about 60 K, the temperature dependence of the resistivity of the sample with $x = 0.02$ obeys simple activation-type equation:

$$\rho = \rho_0 e^{\Delta/2T} \quad (1)$$

where Δ is a transport gap at the Fermi energy. Based on the analysis assuming Eq. (1), Δ is estimated to be 80 meV. This value is consistent with those reported for the single crystal of related half-Heusler semiconductors such as, $\Delta \sim 26$ meV for HfNiSn, 28 meV for TiPtSn, and 79 meV for TiNiSn [4]. However, this estimated value is much smaller than the calculated energy gap ($E_g = 163$ meV [1] or 500 meV [2]).

For the ingots of Fe-doped NiZrSn, comparing with other $C1_b$ semiconductors, such as Mn-doped NiTiSn [14] and Fe-doped CoTiSb [15], it is remarkable that the electrical resistivity shows obvious semiconducting behavior with $x < 0.03$. Although the solubility limit of Fe in NiZrSn is only 2%, the magnetic properties of Fe-doped NiZrSn are worth to investigate. These samples will be expected to become good candidates for the practical application of semiconductor spintronics if the samples show the ferromagnetic property at room temperature.

4. Conclusion

Fe-doped NiZrSn ingots were prepared using arc melting method. Fe can be doped into the $C1_b$ phase of NiZrSn, and the solubility limit of Fe is low, whose value is about 2%. The electrical resistivity shows the semiconducting behavior with $x < 0.03$. Other appropriate methods should be developed in order to prepare the heavily Fe-doped NiZrSn.

References

[1] B.R.K. Nanda, I. Dasgupta, J. Phys.: Condens. Matter 15 (2003) 7307.
[2] S. Öğüt, K.M. Rabe, Phys. Rev. B 51 (1995) 10443.
[3] J. Tobola, J. Pierre, J. Alloys Compd. 269 (2000) 243.
[4] K. Ahilan, M.C. Bennett, M.C. Aronson, N.E. Anderson, P.C. Canfield, E. Munoz-Sandoval, T. Gortenmulder, R. Hendrikx, J.A. Mydosh, Phys. Rev. B 69 (2004) 245116.
[5] K. Kroth, B. Balke, G.H. Fecher, V. Ksenofontov, C. Felser, H.J. Lin, Appl. Phys. Lett. 89 (2006) 202509.
[6] Y. Xia, V. Ponnambalam, S. Bhattacharya, A.L. Pope, S.J. Poon, T.M. Tritt, J. Phys.: Condens. Matter 13 (2001) 77.
[7] F.G. Aliev, N.B. Brandt, V.V. Kozyr'kov, V.V. Moshchalkov, R.V. Skolozdra, Yu.V. Stadnyk, V.K. Pecharskiĭ, JETP Lett. 45 (1988) 684.
[8] C. Uher, J. Yang, S. Hu, D.T. Morelli, G.P. Meisner, Phys. Rev. B 59 (1999) 8615.
[9] Yu.V. Stadnyk, L.P. Romaka, A.M. Goryn, Yu.K. Gorelenko, J. Pierre, R.V. Skolozdra, J. Alloys Compd. 262–263 (1997) 476.
[10] O.I. Bodak, B.V. Padlyak, Yu.V. Stadnyk, J. Pierre, A.V. Tkachuk, L.P. Romaka, Yu.K. Gorelenko, J. Alloys Compd. 317–318 (2001) 357.

[11] Y. Kawaharada, H. Uneda, H. Muta, K. Kurosaki, S. Yamanaka, J. Alloys Compd. 364 (2004) 59.
[12] M.A.S. Boff, G.L. Fraga, D.E. Brandão, A.A. Gomes, T.A. Grandi, Phys. Status Solidi (a) 154 (1994) 549.
[13] I.M. Chapnik, Phys. Status Solidi (b) 113 (1982) K87.
[14] B. Sanyal, O. Eriksson, K.G. Suresh, I. Dasgupta, A.K. Nigam, P. Nordblad, Appl. Phys. Lett. 89 (2006) 212502.
[15] B. Balke, G.H. Fecher, A. Gloskovskii, J. Barth, K. Kroth, C. Felser, R. Robert, A. Weidenkaff, Phys. Rev. B 77 (2008) 045209.